Diagnostic method development when weapons characteristics measuring based on spectral analysis for signals phase shift determination

Vasyl Lytvyn[1,†], Victoria Vysotska[1,†], Sergey Tyshko[2,*,†], Oleksandr Lavrut[3,†], Tetiana Lavrut[3,†] and Mariia Nazarkevych[1,†]

[1] *Lviv Polytechnic National University, S. Bandera 12, 79013Lviv, Ukraine*

[2] *State Scientific Research Institute of Armament and Military Equipment Testing and Certification, 18001 Cherkasy, Ukraine*

[3] *Hetman Petro Sahaidachnyi National Army Academy, Heroes of Maidan 32, 79026Lviv, Ukraine*

Abstract

The analysis of known methods that have found wide application in measuring technology and are designed to control the technical and operational characteristics associated with the measurement of phase shift during the development, manufacture and operation of weapons and military equipment, has been carried out. Based on this analysis, it was determined that measuring systems designed to determine the phase shift of two harmonic signals have two information transmission channels. A measurement task was set to determine the phase shift of two harmonic signals, using the spectral analysis of the signal obtained by summing the harmonic signals after performing their two-semiperiod transformation. The assumptions necessary list for the analytical ratios synthesis, which establishes the relationship between the phase spectra and the amplitudes (power) of the signal obtained by summing harmonic signals after carrying out their two-semiperiod transformation and phase shift of two harmonic signals, are determined. Analytical relations are proposed that establish the relationship between the above-mentioned characteristics. It is shown that the values of the spectrum of phases and amplitudes calculated using the proposed expressions and ratios for calculating the Fourier series coefficients differ by no more than 0.1%. The application of the proposed approach in the artificial intelligence system to diagnose and determine the state of modern weapons and military equipment will allow us to reduce the requirements for measuring equipment without reducing the accuracy of measurements.

Keywords

decision-making system, complex system, phase shift, harmonic signal, spectral analysis

1. Introduction

Today, the Defense Forces of Ukraine actively use various types of weapons and military equipment. An important component of solving the task of effective defence of the state is ensuring the serviceable state of the anti-aircraft defence system, which is part of the units and units of the defence forces, as well as its further modernization, as well as the development of the latest types of weapons. The assessment of the technical condition of the weapons and military equipment (WME) sample, or the decision on admission to the supply of the latest weapons to the Armed Forces, is made based on tests, by analyzing its technical characteristics for compliance with regulatory and technical documents (technical task, technical conditions, operating instructions, repair documentation sets). Defects are an important technological operation during the capital repair works of WME. As you know, the task of this technological operation is to determine the possibility of using components from the composition of the sample subject to restoration. For mechanical components, various parameters are measured, including geometric dimensions, and physical and chemical properties of the material. To reduce the time and increase the accuracy of measurements, predicting the state of the WME, it is necessary to use intelligent diagnostic systems [16]. The use of artificial intelligence in such systems for processing measurement results, and forecasting (simulation) of the future state of WME is an integral component of the development of this field. The measurement of the above-mentioned characteristics of small arms, artillery and missile-artillery weapons, and wheeled and tracked military equipment is based on non-destructive control methods. Non-destructive control methods include radiography, ultrasonic flaw detection, magnetic resonance research methods, and others. Measuring systems that implement the specified measurement methods widely use phaseometry methods [1, 2, 17, 34]. Also, phase measurement methods are widely used in radar and radio navigation, aviation and space engineering, geodesy, mechanical engineering, communication and many other fields [7, 21-27]. The phase-measuring transformation of various physical processes into the phase shift of harmonic signals ensures high metrological characteristics. Therefore, phaseometry, as a method of transformation and measurement, has long gone beyond the traditional use in radio engineering, navigation and communication and is successfully used in experimental physics, radio physics, experimental medicine, modern fields of science and technology when carrying out precision measurements [3-5, 13-15, 17-20, 37-39]. Based on the above, in [2, 5], a list of WME parameters, which should be converted into a phase shift when measured during sample manufacturing and testing, is defined. These parameters can include: electrical and magnetic conductivity, permeability, geometric dimensions, movement parameters, microdisplacement, capacity, element inductance, liquid level, liquid or gas consumption, angle of rotation, speed of rotation, electric voltage and current, temperature, distance, angle, delay time. Thus, conducting scientific research to find new principles for determining the phase shift, which will allow to reduce the cost of performing work on the control of the characteristics of the latest and modernized weapons at the stages of development and production, is relevant.

2. Related works

For harmonic signals, such concepts as phase, initial phase, phase shift and delay time are used in measuring technology. The most complete classification of methods for measuring phase shifts of harmonic signals is given in works [2, 5, 6, 13, 14, 15].

According to the principle of measurement, the methods of phaseometry are divided into compensatory methods and methods of converting the phase shift into other values - voltage, time interval, and geometric parameters of oscillographic images of the investigated signals. These methods differ from each other in technical implementation, complexity and accuracy. Compensation methods [2, 5, 6, 13, 14] are based on the process of balancing (compensating) the phase shift $\Delta\varphi \in [0, 2\pi)$ between the measured harmonic signals, that is, reducing the phase shift to zero by adjusting the phase of one of the signals using an adjustable phase shifter (measures of phase shift). This method ensures the achievement of high measurement accuracy, close to the accuracy of a phase shifter. Measurement methods based on the transformation of the phase shift into other signals [2, 5, 6, 13, 14, 15] allow determining the value of the phase shift of the signals after their transformation into other intermediate values that are convenient to use for measurement. These intermediate values include voltage, current, displacement of the electron beam of the oscilloscope, and time values. The disadvantages of known methods include [2, 5, 6]:

- a significant impact on the accuracy of measuring the phase shift of the error component, which is caused by the phase asymmetry of the signal transmission channels;
- the presence of two channels for conducting analogue-to-digital conversion of input signals, which leads to the need for mutual synchronization of the frequency of clock generators for each of the channels;
- significant impact on the accuracy of external and internal noise measurement;
- non-linear nature of the scale.

At present, one of the effective and widespread ways of reducing the impact of external and internal noise on the quality of solving problems of analyzing and processing signals of various natures is the use of spectral analysis [35-36]. As is known, a periodic signal of any form can be decomposed into harmonic signals whose frequencies are multiples of the frequency (period) of the analyzed signal. A similar research method is called spectral analysis, the mathematical basis of which is the Fourier series [8, 31-33].

Fourier series of arbitrary periodic signals can contain an infinitely large number of terms. One of the advantages of the Fourier transform is that when limiting the Fourier series to any finite number of its terms, it provides the best mean square error of approximation to the original function (for a given number of terms). The convenience of using the frequency representation of signals lies in the fact that harmonic functions are eigenfunctions of operations of transfer, integration, differentiation and other linear operations invariant in coordinates. They pass through linear systems without changing the shape and frequency of the harmonics, only the initial phase and amplitude of the

oscillations change. In the general case, when expanding into a Fourier series of a periodic signal with a period T_s, it is possible to use an interval $\left[-\dfrac{T_c}{2}, \dfrac{T_c}{2}\right]$.

If we denote the angular frequency through ω_c then since $\omega_c = \dfrac{2\pi}{T_c}$, then for the function $f(t)$ on the interval $\left[-\dfrac{T_c}{2}, \dfrac{T_c}{2}\right]$, the Fourier series has the form:

$$f(t) = \frac{a_0}{2} + \sum_{k=1}^{n}\{a_k \cos \omega_c kt + b_k \sin \omega_c kt\}. \tag{1}$$

Expressions for determining the coefficients of the Fourier series a_k, b_k have the form:

$$a_k = \frac{2}{T_c}\int_{-\frac{T_c}{2}}^{\frac{T_c}{2}} f(t)\cos \omega_c kt\, dt, \quad (k = 0,1,2,\ldots,n) \tag{2}$$

$$b_k = \frac{2}{T_c}\int_{-\frac{T_c}{2}}^{\frac{T_c}{2}} f(t)\sin \omega_c kt\, dt \quad (k = 1,2,\ldots,n). \tag{3}$$

Series (1) represents the decomposition of the periodic signal f(t) into the sum of real elementary harmonic functions (cosine and sine) with weighting coefficients, the geometric sum of whose values (that is, the values of a_k and b_k are nothing but the real amplitudes of the corresponding harmonic oscillations with frequencies $k\omega_c$. The set of amplitude values of these harmonics forms a one-sided physically real (only for positive frequencies $k\omega_c$ signal spectrum.

The goal of the work. To propose the scientific and technical basis of the alternative principle of determining the phase shift, the mathematical basis of which is possible to consider analytical relations that establish the relationship between the phase shift of two harmonic signals and the spectral characteristics of the signal obtained when summing them after carrying out a two-semiperiod transformation, which will allow to significantly reduce the error component, due to the phase asymmetry of the signal transmission channels and the influence of external and internal noise during monitoring of the characteristics (parameters) of the WME.

3. Methods and models

At present, the determination of the phase shift is of greatest interest to phasometry. Phase shift [9, 28-30] refers to the modulus of the difference between the initial phases of two harmonic signals of the same frequency. As a rule, the measurement of phase shifts of signals is based on the model of a harmonic signal, which is specified without changes in its parameters over an infinite time interval. This model is ideal, and in practice, a model with a finite time window is used, that is, measurements are carried out on a finite time interval.

Then, based on the above, we will formulate the problem of determining the phase shift using the spectral analysis of the signal obtained as a result of the summation of two harmonic signals, after carrying out their two-half-period transformation. Let's consider the initial data necessary to solve the specified measurement problem.

Let there be two harmonic signals $u_1(t)$ and $u_2(t)$, which have a phase shift relative to the other equal to $\Delta\varphi$, in the interval from 0 to 2π. Based on the fact that phase shift

measurements refer to relative measurements, the mathematical record of changes in signals $u_1(t)$ and $u_2(t)$ can be represented in the form:

$$u_1(t) = U_{m1} \cos(2\pi f t), \tag{4}$$
$$u_2(t) = U_{m2} \cos(2\pi f t + \Delta\varphi),$$

where U_{m1} is signal amplitude $u_1(t)$; U_{m2} is signal amplitude $u_2(t)$; $f = 1/T$ is signal frequency; T is signal period.

The module is extracted from signals $u_1(t)$ and $u_2(t)$, as a result of which we get:

$$u_1'(t) = |u_1(t)| = |U_{m1} \cos(2\pi f t)|, \tag{5}$$
$$u_2'(t) = |u_2(t)| = |U_{m2} \cos(2\pi f t + \Delta\varphi)|,$$

After summing the signals $u_1'(t)$ and $u_2'(t)$, we get:

$$u_\Sigma' \tag{6}$$
$$= \begin{cases} U_{1min} + \dfrac{U_{1min} - U_{2min}}{t_{1.2}} t + \left(U_{1max}' - \dfrac{U_{1min} + U_{2min}}{2} \right) \sin\left(\left(2f - \dfrac{2\pi f}{\Delta\varphi} \right) t \right), & t_1 \leq t < t_2 \\[4mm] U_{2min} + \dfrac{U_{2min} - U_{1min}}{t_{2.3}} t + \left(U_{2max}' - \dfrac{U_{2min} + U_{1min}}{2} \right) \sin\left(\left(\dfrac{2\pi f}{\Delta\varphi} \right) t \right), & t_2 \leq t < t_1 \end{cases}$$

where: U_{1min} and U_{2min} are breakpoints of the function on the interval from 0 to $\dfrac{T}{2}$;

$U_{1max}' = (U_{m1} + U_{m2}) \cos\dfrac{\Delta\varphi}{2}$ is local maximum on the time interval $t_{1.2} = \dfrac{1}{2f} - \dfrac{\Delta\varphi}{2\pi f}$;

$U_{2max}' = (U_{m1} + U_{m2}) \sin\dfrac{\Delta\varphi}{2}$ is local maximum on the time interval $t_{2.1} = \dfrac{\Delta\varphi}{2\pi f}$.
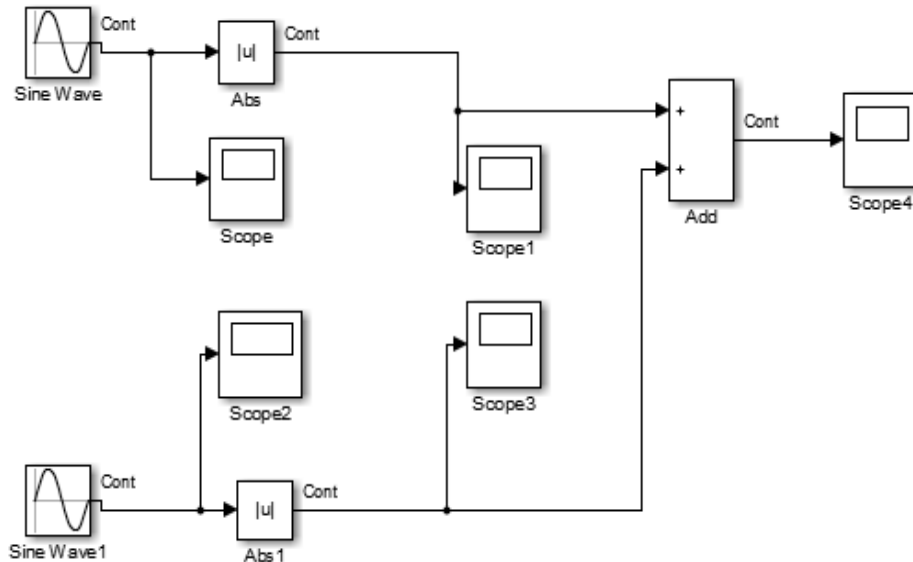

Figure 1: Structural diagram of the transformation of signals into a signal

Synthesis of time diagrams that describe the order of formation of the signal $u_\Sigma^/$ (t) using relations (4) and (5) will be carried out in the Matlab environment using the Simulink tool application. To do this, we synthesize the scheme shown in Fig. 1. In this scheme, the synthesis of signal $u_1(t)$ is carried out by the harmonic signal generator "Sine Wave", and the signal $u_2(t)$ by the generator "Sine Wave 1". From the "Sine Wave" output, the signal enters the "Abs" block and the oscilloscope marked "Scope", which is designed to form the time diagram of the $u_1(t)$ signal. According to the "Sine Wave 1" output, the signal enters the "Abs 1" block and the oscilloscope marked "Scope 2", which is designed to form the timing diagram of the $u_2(t)$ signal. At the output of the "Abs" block, a signal $u_1^/(t)$ is formed, which is fed to the first input of the summation device "Add" and "Scope 1". "Scope 1" forms a time diagram of the signal $u_1^/(t)$. Similarly, at the output of the "Abs 1" block, a signal $u_2^/(t)$ is formed, which is fed to the second input of the summation device "Add" and "Scope 3", which forms a time diagram of the signal $u_2^/(t)$. At the output of the "Add" block, we will receive the signal $u_\Sigma^/$ (t). The signal u_Σ^- (t) is fed to "Scope 4", which will form its signal time diagram

4. Experiments, results and discussion

Fig. 2 shows the time diagrams of the signals $u_1(t)/u_2(t)$, $u_1^/(t)/u_2^/(t)$ and $u_\Sigma^/(t)$ at the value $\Delta\varphi = 0$, as well as the "Sine Wave" generator settings tab " and "Sine Wave1".
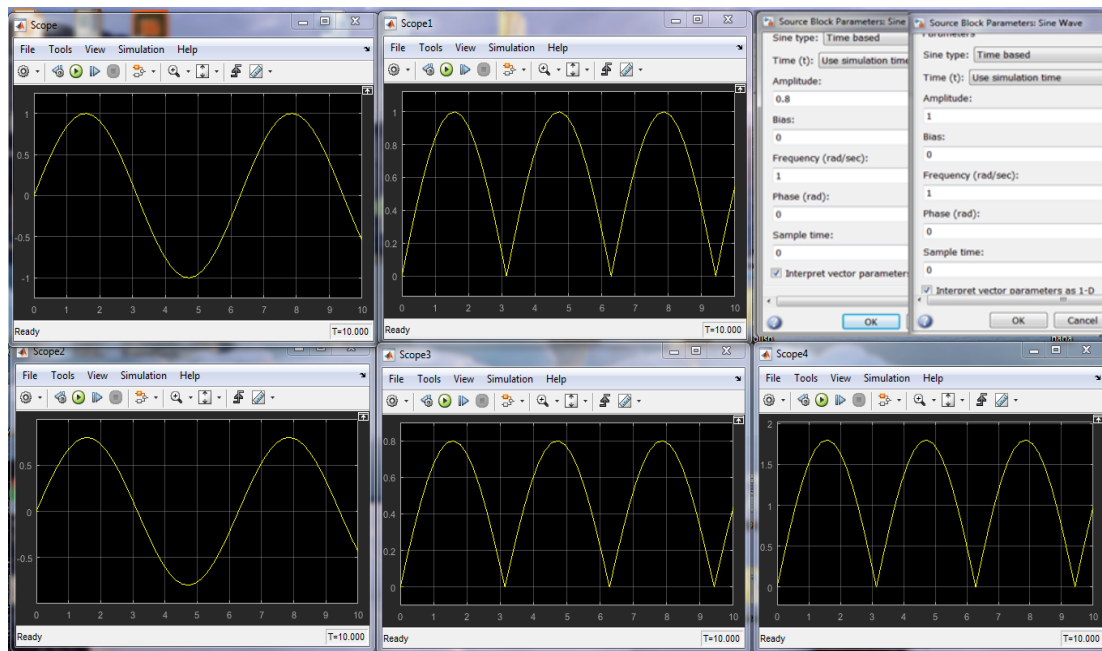

Figure 2: Time diagrams of signals $u_1(t)$ and $u_2(t)$,, $u_1^/(t)$ and $u_2^/(t)$, and $u_\Sigma^/(t)$ at the value of $\Delta\varphi = 0$

According to the settings tabs, generators "Sine Wave" generates a sinusoidal signal with an amplitude equal to 1, and "Sine Wave1" with an amplitude equal to 0.8, other settings of the tabs are as follows: the constant component of the signals is 0, the frequency of the signal is 1 rad/s, the initial phase of the signals is 0 rads, the quantization time is minimal for this device, i.e. 0 on the tab. The timing diagram shown on "Scope" and "Scope 2" fully confirms the settings on the tab. The time diagrams for the $u_{\Sigma}^{/}$ (t) signal are shown on the "Scope 4" tab. The analysis of this time diagram shows that the signal $u_{\Sigma}^{/}$ (t) has a period equal to π s, the maximum value is equal to 1.8, and the minimum value is equal to 0. The obtained results correspond to the summation of two harmonic signals, after carrying out their two-and-a-half period transformation.

Fig. 3 shows the time diagrams of signals $u_1(t)$ and $u_2(t)$, $u_1^{/}(t)$ and $u_2^{/}(t)$ and $u_{\Sigma}^{/}(t)$, at the value of $\Delta\varphi = 0,9$ rad, as well as the generator settings tab "Sine Wave" and "Sine Wave1". According to the configuration tabs, the "Sine Wave" generator generates a sinusoidal signal with an amplitude equal to 1, the constant component of the signal is 0, the frequency of the signal is 1 rad/s, the initial phase of the signal is 0 rad, the quantization time is minimal for this device, i.e. 0 on the tab.

Figure 3: Time diagrams of signals $u_1(t)$ and $u_2(t)$,, $u_1^{/}(t)$ and $u_2^{/}(t)$, and $u_{\Sigma}^{/}(t)$ at the value of $\Delta\varphi = 0.9$ rad

According to the settings tabs, the "Sine Wave1" generator generates a sinusoidal signal with an amplitude equal to 0.8, the constant component of the signal is 0, the frequency of the signal is 1 rad/s, the initial phase of the signal is 0.9 rad, the quantization time is minimal for this device, i.e. 0 at tab. The time diagrams for signals $u_1^{/}(t)$ and $u_2^{/}(t)$ are shown in the "Scope 1" and "Scope 3" tabs. The analysis of the data of the time diagrams shows that they

have a period equal to π s, the maximum values of $u_1^/(t)$ are equal to 1, and $u_2^/(t)$ is 0.8, also the $u_2^/(t)$ signal precedes the $u_1^/(t)$ about 0.9. The time diagrams for the $u_\Sigma^/$ (t) signal is shown on the "Scope 4" tab. Analysis of this time diagram shows that the signal $u_\Sigma^/$ (t) has a period equal to π s. In the time interval from 0 to (π-0.9) s, the maximum value is approximately 1.65, and the minimum value is approximately 0.78. In the time interval from $(\pi - 0{,}9)$ to π, the maximum value is approximately 0.8, and the minimum value is 0.6.

Fig. 4 shows the time diagrams of the signals $u_1(t)/u_2(t)$, $u_1^/(t)/u_2^/(t)$, and $u_\Sigma^/(t)$ at the value of $\Delta\varphi = 1.2$ rad, as well as the tab for setting the generator "Sine Wave"/"Sine Wave1".
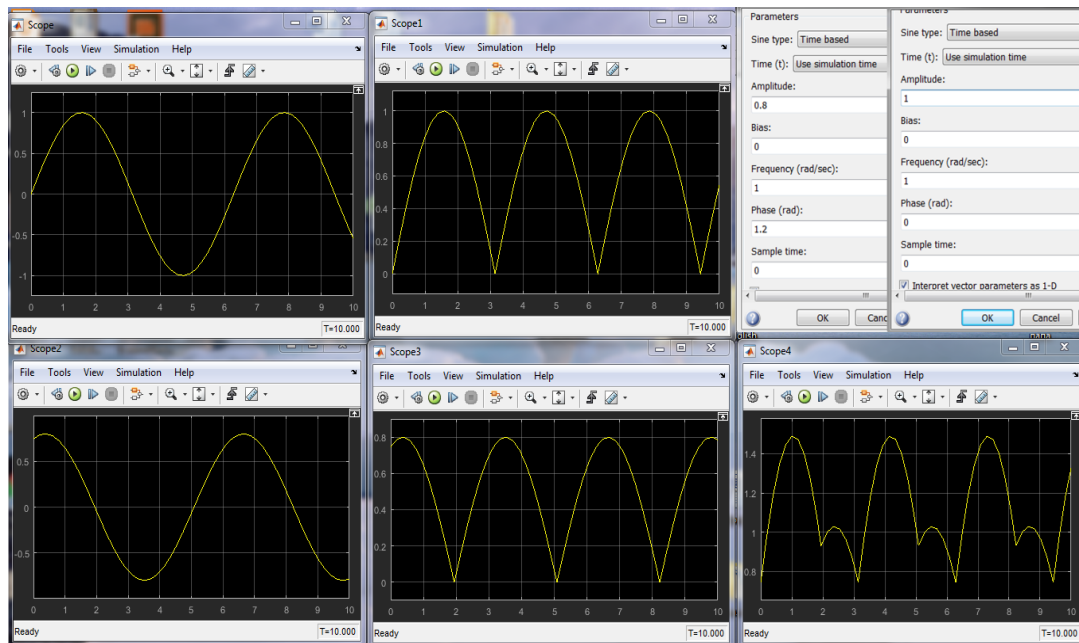
Figure 4: Time diagrams of signals $u_1(t)$ and $u_2(t)$, $u_1^/(t)$ and $u_2^/(t)$, and $u_\Sigma^/(t)$ at Δφ=1.2 rad

According to the configuration tabs, the "Sine Wave" generator generates a sinusoidal signal with an amplitude equal to 1, the constant component of the signal is 0, the frequency of the signal is 1 rad/s, the initial phase of the signal is 0 rad, the quantization time is minimal for this device, i.e. 0 on the tab. According to the settings tabs, the "Sine Wave1" generator generates a sinusoidal signal with an amplitude equal to 0.8, the constant component of the signal is 0, the frequency of the signal is 1 rad/s, the initial phase of the signal is 1.2 rad, the quantization time is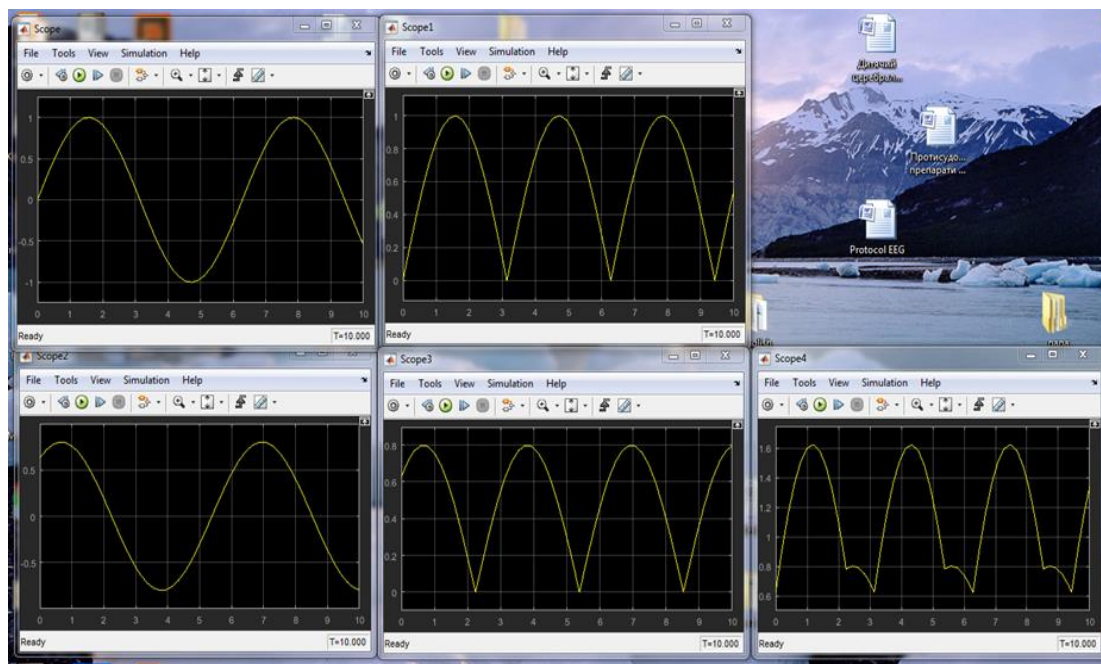 minimal for this device, i.e. 0 on the tab. The time diagrams for signals $u_1^/(t)$ and $u_2^/(t)$ are shown in the "Scope 1" and "Scope 3" tabs. The analysis of the data of the time diagrams shows that they have a period equal to π s, the maximum values of $u_1^/(t)$ are equal to 1, and $u_2^/(t)$ is 0.8, also the $u_2^/(t)$ signal precedes the

$u_1^/(t)$ about 1.2 rad. The time diagrams for the $\overline{u_\Sigma}$ (t) signal are shown on the "Scope 4" tab. Analysis of this time diagram shows that the signal $u_\Sigma^/$ (t) has a period equal to π s. In the time interval from 0 to $(\pi - 1.2)$ s, the maximum value is approximately 1.5, and the

minimum value is 0.95. In the time interval from $(\pi - 1.2)$ to π, the maximum value is approximately 1.05, and the minimum value is 0.75.

From Fig. 4, it can be seen, and it is also shown in [10, 11] that $u_{\Sigma}^{/}$ (t) depending on the value of $\Delta\varphi$ of the input signals $u_1(t)$ and $u_2(t)$:

- is a periodic signal with a period of $T' = \dfrac{1}{2f} == \dfrac{T}{2}$;
- has two local maxima U_{1max} and U_{2max}, which correspond to the moments of t_{1max}, t_{2max} and two breaks U_{1min} and U_{2min}, which correspond to the moments of time t_1, t_2, respectively;
- a change in the value of the phase shift angle $\Delta\varphi$ leads to a change in the values of U_{1max}, U_{2max}, U_{1min} end U_{2min} and time parameters t_{1max}, t_{2max} end t_2.

A change in the values of the above characteristics of the signal $u_{\Sigma}^{/}$ (t) leads to a change in its shape, which in turn will lead to a change in the values of the coefficients a_k and b_k of the Fourier series depending on the change in the magnitude of the phase shift $\Delta\varphi$.

When conducting spectral analysis, such concepts as amplitude spectrum, power spectrum and phase spectrum are used. When conducting spectral analysis, such concepts as amplitude spectrum, power spectrum and phase spectrum are used. According to [12], the spectrum of amplitudes is understood as the set of absolute values of the coefficients C_k $(k = 0,1,2,\ldots,n)$, which are determined from the known values of a_k and b_k by the ratio:

$$|C_k| = \frac{\sqrt{a_k^2 + b_k^2}}{2}. \tag{7}$$

The value $|C_k|$ indicates the value of the amplitude of the k-th harmonic signal when expanded into a Fourier series. The power spectrum is understood as a set of arguments of the values $|C_k|^2$. The spectrum of phases means the set of arguments $\angle C_k$ $(k = 0,1,2,\ldots,n)$, which are determined by the known values of a_k and b_k by the ratio:

$$\angle C_k = arctg\,\frac{b_k}{a_k}. \tag{8}$$

The value of $\angle C_k$ indicates the value of the initial phase of the k-th harmonic signal when expanded into a Fourier series. Then, based on the above, we will formulate the task of determining the phase shift using Fourier series decomposition, as a synthesis of analytical relations that describe the relationship between the change in the spectrum of amplitudes (power) and the spectrum of the phases of the signal $u_{\Sigma}^{/}$ (t) depending on the change in $\Delta\varphi$. Synthesis of relations that determine the relationship between the value of $\Delta\varphi$ and the characteristics of the spectrum of amplitudes (power) and the spectrum of phases of the signal $u_{\Sigma}^{/}$ (t) using the following assumptions. As can be seen from (4), the signal $u_{\Sigma}^{/}$ (t) is formed by summing two signals $u_1^{/}(t)$ and $u_2^{/}(t)$. These signals are formed by signals $u_1(t)$ and $u_2(t)$, while the amplitude of U_{m1} differs from the amplitude of U_{m2} by v times, and have a phase shift $\Delta\varphi$.

Then it can be stated that the signal $u_1(t)$ precedes the signal $u_2(t)$ by a certain time interval τ, i.e. $u_2(t) = v u_1(t - \tau)$. According to the known values of $\Delta\varphi$ and T, the time interval τ is determined by the ratio:

$$\tau = \frac{\Delta\varphi}{2\pi} \text{T}. \tag{9}$$

As shown in [12], the shift of the signal in the time domain by some interval τ leads to a change in the phase spectrum, but the spectrum of the signal amplitudes remains unchanged. Taking into account expressions (7) and (8) provided that $U_{m1.k}$ and $U_{m2.k}$ are the amplitude values of the k-th harmonics of signals $u_1'(t)$ and $u_2'(t)$, respectively, and $\varphi_{1.к}$ and $\varphi_{2.к}$ values of the initial phases of the k-th harmonics of the signals $u_1'(t)$ and $u_2'(t)$, respectively, the Fourier series for the signal u_Σ' (t) will have appearance:

$$u_\Sigma' \ (t) = U_{m1.0} + \sum_{k=1}^{n}[U_{m1.k} \sin(2\omega kt + \varphi_{1.k})] + U_{m2.0} + \tag{10}$$

$$+ \sum_{k=1}^{n}[U_{m2.k} \sin(2\omega kt + \varphi_{2.k})] =$$

$$= (U_{m1.0} + U_{m2.0}) + [U_{m1.1} \sin(2\omega t + \varphi_{1.1}) + U_{m2.1} \sin(2\omega t + \varphi_{2.1})] +$$

$$+ [U_{m1.2} \sin(4\omega t + \varphi_{1.2}) + U_{m2.2} \sin(4\omega t + \varphi_{2.2})] + \cdots +$$
$$+ [U_{m1.n} \sin(2n\omega t + \varphi_{1.n}) + U_{m2.n} \sin(2n\omega t + \varphi_{2.n})]$$

To synthesize analytical relations for determining the values of the amplitude $U_{m\Sigma 1}'$ and the initial phase $\varphi_{m\Sigma 1}'$ of the first harmonic of the signal u_Σ' (t), we will construct the vector diagram of the first harmonics of the signals $u_1'(t)$ and $\overline{u_2'}(t)$ in the presence of a phase shift equal to $\Delta\varphi$ of the signals $u_1(t)$ and $u_2(t)$, provided that the initial phase of the signal $u_1(t)$ is zero, taking into account the following remarks and assumptions:

- it is known that the frequency of the first harmonic of the signal is equal to the frequency of the signal;
- it is shown in [10, 11] and it can be seen in Figs. 2...4 that $u_1'(t)$, $u_2'(t)$ and u_Σ' (t) have a period that is two times shorter than $u_1(t)$ and $u_2(t)$;
- it can be asserted that $u_2(t) = v u_1(t - \tau)$ and $u_2'(t) = v u_1'(t - \tau)$, that is, the time interval of the shift τ between the signals $u_1'(t)$ and $u_2'(t)$, and the shift time interval τ between signals $u_1(t)$ and $u_2(t)$ is the same;
- based on relation (9) and the above remarks, it can be seen that the value of the phase shift of the first harmonics of signals $u_1'(t)$ and $u_2'(t)$ will be equal to $2\Delta\varphi$, if there is a phase shift equal to $\Delta\varphi$ of signals $u_1(t)$ and $u_2(t)$.

The above vector diagram is shown in Fig. 5. From Fig. 5, it can be seen that for the calculation of the values of the characteristics of the vector of the first harmonic of the signal u_Σ' (t) according to the vectors of the first harmonics of the signals $u_1'(t)$ and $u_2'(t)$, the parallelogram method was used.
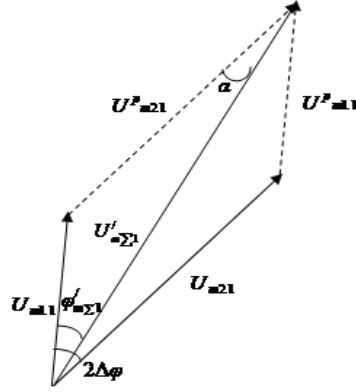
Figure 5: Vector diagram for determining the value of the initial phase $\varphi'_{m\Sigma 1}$ of the first harmonic of the signal $u'_\Sigma (t)$

Thus, the value of the amplitude $U'_{m\Sigma 1}$ of the first harmonic of the signal $u'_\Sigma (t)$ according to the known values of the amplitudes of the first harmonics $U_{m1.1}$ and $U_{m2.1} = U^3{}_{m2.1}$ of the signals $u'_1(t)$ and $u'_2(t)$ in the presence of a phase shift equal to $\Delta\varphi$ of signals $u_1(t)$ and $u_2(t)$ is determined by the ratio:

$$U'_{m\Sigma 1} = \sqrt{U^2{}_{m1.1} + U^2{}_{m2.1} + 2U_{m1.1}U_{m2.1}\cos 2\,\Delta\varphi} \tag{11}$$

Then the value of the amplitude $U'_{m\Sigma k}$ of the k-th harmonic of the signal $u'_\Sigma (t)$ according to the known values of the amplitudes $U_{m1.k}$ and $U_{m2.k}$ of the k-th harmonics of the signals $u'_1(t)$ and $u'_2(t)$ at a phase shift value equal to $\Delta\varphi$ of signals $u_1(t)$ and $u_2(t)$ is calculated using the ratio:

$$U'_{m\Sigma k} = \sqrt{U^2{}_{m1.k} + U^2{}_{m2.k} + 2U_{m1.k}U_{m2.k}\cos 2\,k\Delta\varphi}. \quad (k = 0,1,2,\ldots,n) \tag{12}$$

The synthesis of analytical ratios for calculating the values of $U_{m1.k}$ will be carried out in the following order. Let's determine the spectrum of amplitudes for the signal $u'_1(t)$ under the condition $U_{m1} = 1$. The relations for calculating the coefficients of the Fourier series $a_{1.k}$ и $b_{1.k}$ of the signal $u'_1(t)$ are as follows:

$$a_{1.k} = \frac{2}{T'}\int_{-\frac{T'}{2}}^{\frac{T'}{2}}|\cos(\omega t)|\cos(2\omega kt)dt. \quad (k = 0,1,2,\ldots,n) \tag{13}$$

$$b_{1.k} = \frac{2}{T'}\int_{-\frac{T'}{2}}^{\frac{T'}{2}}|\cos(\omega t)|\sin(2\omega kt)dt, \quad (k = 1,2,\ldots,n) \tag{14}$$

Based on the known values of $a_{1.k}$ and $b_{1.k}$, the value of $U_{m1(1).k}$ is calculated by the ratio:

$$U_{m1(1).k} = \frac{\sqrt{a_{1.k}^2 + b_{1.k}^2}}{2}. \tag{15}$$

The values of $U_{m1(1).k}$ were calculated using the universal mathematical package MathCAD, the results are presented in Fig. 6. Using the property of the linearity of the Fourier series, the relationship for determining the value of the amplitude $U'_{m\Sigma k}$ k-th harmonic of the signal u'_{Σ} (t) based on the known values of the amplitudes U_{m1} and U_{m2} at the value of the phase shift of the initial signals $u_1(t)$ and $u_2(t)$, which is equal to $\Delta\varphi$, is calculated using the relationship:

$$U'_{m\Sigma k} = U_{m1(1).k}\sqrt{U^2_{m1.} + U^2_{m2.} + 2U_{m1.}U_{m2.}\cos 2\,k\Delta\varphi}, \ (k = 0,1,2,\ldots,n) \qquad (16)$$

To synthesize analytical relations to determine the values of the initial phase $\varphi'_{m\Sigma 1}$ of the first harmonic of the signal u'_{Σ} (t), we will use the theorem of sines for the triangle formed by the sides $U_{m1.1}$, $U^p_{m2.1}$ and $U'_{m\Sigma 1}$ on the vector diagram of the first harmonics of the signals $u'_1(t)$ and $u'_2(t)$ in the presence of a phase shift equal to $\Delta\varphi$ of the signals $u_1(t)$ and $u_2(t)$, we write

$$\frac{U_{m1.1}}{sin(\alpha)} = \frac{U^p{}_{m1.1}}{sin\left(\varphi'_{m\Sigma 1}\right)}$$

Solving this equation relative to $\varphi'_{m\Sigma 1}$ based on the fact that

$$U_{m1.1} = U_{m1(1).1}U_{m1},$$
$$U^p_{m2.1} = U_{m2.1} = U_{m1(1).1}U_{m2},$$
$$\alpha = 2\Delta\varphi - \varphi'_{m\Sigma 1}.$$

We obtain that the value of the initial phase $\varphi'_{m\Sigma 1}$ of the first harmonic of the signal u'_{Σ} (t) depending on the value of $\Delta\varphi$ is determined by the following relation, provided that the initial phase of the signal u_1 (t) is zero

$$\varphi'_{m\Sigma 1} = arcctg\left[\cos e\, c(2\Delta\varphi)\cdot\left(\frac{U_{m1}}{U_{m2}} + \cos(2\Delta\varphi)\right)\right] \qquad (17)$$

$$U_{m1(1).k} =$$

	0
0	0.637
1	0.212
2	0.042
3	0.018
4	0.01
5	$6.431\cdot 10^{-3}$
6	$4.452\cdot 10^{-3}$
7	$3.265\cdot 10^{-3}$
8	$2.497\cdot 10^{-3}$
9	$1.971\cdot 10^{-3}$

Figure 6: The value of $U_{m1(1).k}$ for $U_{m1} = 1B$

Taking into account (9), for the kth harmonic, the initial phase $\varphi'_{m\Sigma k}$ on the interval $\left[-\pi/2, \pi/2\right]$ of the signal u'_{Σ} (t) will be equal to:

$$\varphi'_{m\sum k} = arcctg \left[cos\,e\,c(2k\Delta\varphi) \cdot \left(\frac{U_{m1}}{U_{m2}} + cos(\,2k\Delta\varphi)\right)\right], (k = 0,1,2,\ldots,n) \qquad (18)$$

Let us consider the possibility of using the obtained relations for the synthesis of the spectrum of amplitudes and phases of the signal $u'_{\sum}$ (t). To do this, let's compare the spectrum of amplitudes and phases of the signal $u'_{\sum}$ (t) obtained using relations (17) and (18) and the following expressions:

$$a_k = \frac{2}{T'}\int_{-\frac{T'}{2}}^{\frac{T'}{2}}[|U_{m1}\,cos(\,\omega t)| + |U_{m2}\,cos(\,\omega t + \Delta\varphi)|]\,cos\,2\,\omega ktdt,\,(k = 0,1,2,\ldots,n) \qquad (19)$$

$$b_k = \frac{2}{T'}\int_{-\frac{T'}{2}}^{\frac{T'}{2}}[|U_{m1}\,cos(\,\omega t)| + |U_{m2}\,cos(\,\omega t + \Delta\varphi)|]\,sin\,2\,\omega ktdt,\,\,(k = 1,2,\ldots,n) \qquad (20)$$

$$U_{m.k} = \frac{\sqrt{a_{1.k}^2 + b_{1.k}^2}}{2}, \quad \angle C_k = arctg\,\frac{b_k}{a_k}. \qquad (21)$$

As an indicator of approximation of the spectrum of amplitudes, we use the difference between the value of $U'_{m\sum k}$ obtained using relation (16) and the value of $U_{m.k}$ calculated using relations (19-21). The calculations were performed in the MathCAD mathematical package, and the comparison results for some values of $\Delta\varphi$, U_{m1} and U_{m2} are presented in Fig. 7a. These results show that the relative deviation of the amplitude spectrum obtained using (17) differs from the values of the amplitude spectrum obtained using (19 ... 21) less than 0.1%. As an indicator of approximation of the phase spectrum, we use the difference between the value of $\varphi'_{m\sum k}$ obtained using relation (18) and the value of $\angle C_k$ in the interval $[-\pi/2,\pi/2]$ calculated using relation (19, 20, 21).

The results of the comparison for some values of $\Delta\varphi$ are presented in Fig. 7b. These results show that the relative deviation of the phase spectrum obtained using (19) differs from the values of the phase spectrum obtained using (19, 20, 21) by less than 0.1%.

5. Conclusions

An analysis of the known principles of measuring phase shifts was carried out. The analysis showed that a significant contribution to the final measurement error of phase shifts is made by the component caused by the phase asymmetry of signal transmission channels and the influence of external and internal noise. As an alternative approach to determining the phase shift, it is proposed to use a signal obtained as a result of summing harmonic signals after carrying out their two-semiperiod transformation followed by its spectral analysis. Analytical relations are proposed that establish the relationship between the phase shift and the characteristics of the spectrum of amplitudes and phases of the considered signal. The adequacy of the proposed analytical ratios was checked. As a result of the verification, it was established that the relative discrepancy between the characteristics of the spectrum obtained using the proposed ratios and using the ratios for calculating the coefficients of the Fourier series does not exceed 0.1%.

Part a) — $\Delta(n)$, $Um1 := 0.6$, $Um2 := 0.5$

n	$\Delta\phi := 0.1$	$\Delta\phi := 0.5$	$\Delta\phi := 0.9$
0	$-3.094 \cdot 10^{-6}$	$2.336 \cdot 10^{-6}$	$-2.998 \cdot 10^{-6}$
1	$2.824 \cdot 10^{-6}$	$-3.933 \cdot 10^{-5}$	$-1.939 \cdot 10^{-7}$
2	$-1.356 \cdot 10^{-6}$	$4.928 \cdot 10^{-7}$	$1.051 \cdot 10^{-7}$
3	$-2.866 \cdot 10^{-6}$	$-1.181 \cdot 10^{-6}$	$2.078 \cdot 10^{-7}$
4	$6.416 \cdot 10^{-7}$	$1.787 \cdot 10^{-7}$	$2.109 \cdot 10^{-7}$
5	$-1.098 \cdot 10^{-5}$	$-4.644 \cdot 10^{-5}$	$3.526 \cdot 10^{-8}$
6	$-1.414 \cdot 10^{-5}$	$-7.347 \cdot 10^{-7}$	$3.793 \cdot 10^{-6}$
7	$-7.073 \cdot 10^{-7}$	$-6.875 \cdot 10^{-7}$	$2.22 \cdot 10^{-7}$
8	$9.643 \cdot 10^{-8}$	$2.184 \cdot 10^{-8}$	$-2.663 \cdot 10^{-9}$
9	$-1.788 \cdot 10^{-7}$	$-8.304 \cdot 10^{-7}$	$2.186 \cdot 10^{-7}$

$\Delta(n)$, $Um1 := 0.8$, $Um2 := 0.6$

n	$\Delta\phi := 0.1$	$\Delta\phi := 0.5$	$\Delta\phi := 0.9$
0	$-3.713 \cdot 10^{-6}$	$2.803 \cdot 10^{-6}$	$-3.597 \cdot 10^{-6}$
1	$3.414 \cdot 10^{-6}$	$-4.782 \cdot 10^{-5}$	$-2.427 \cdot 10^{-7}$
2	$-1.537 \cdot 10^{-6}$	$6.659 \cdot 10^{-7}$	$1.183 \cdot 10^{-7}$
3	$-3.243 \cdot 10^{-6}$	$-8.923 \cdot 10^{-7}$	$2.459 \cdot 10^{-7}$
4	$-8.655 \cdot 10^{-6}$	$1.156 \cdot 10^{-6}$	$2.497 \cdot 10^{-7}$
5	$-1.276 \cdot 10^{-5}$	$-6.936 \cdot 10^{-7}$	$1.212 \cdot 10^{-8}$
6	$-1.156 \cdot 10^{-5}$	$-8.426 \cdot 10^{-7}$	$4.822 \cdot 10^{-6}$
7	$-2.57 \cdot 10^{-7}$	$-2.402 \cdot 10^{-6}$	$2.753 \cdot 10^{-7}$
8	$1.242 \cdot 10^{-7}$	$4.431 \cdot 10^{-8}$	$-2.988 \cdot 10^{-8}$
9	$-2.235 \cdot 10^{-7}$	$-8.075 \cdot 10^{-7}$	$1.758 \cdot 10^{-7}$

$\Delta(n)$, $Um1 := 1.1$, $Um2 := 0.6$

n	$\Delta\phi := 0.1$	$\Delta\phi := 0.5$	$\Delta\phi := 0.9$
0	$2.066 \cdot 10^{-5}$	$2.803 \cdot 10^{-6}$	$-3.597 \cdot 10^{-6}$
1	$3.486 \cdot 10^{-6}$	$-1.504 \cdot 10^{-6}$	$-2.654 \cdot 10^{-7}$
2	$-1.272 \cdot 10^{-6}$	$8.45 \cdot 10^{-7}$	$9.235 \cdot 10^{-8}$
3	$-2.67 \cdot 10^{-6}$	$-2.672 \cdot 10^{-7}$	$2.351 \cdot 10^{-7}$
4	$-7.756 \cdot 10^{-6}$	$1.003 \cdot 10^{-6}$	$2.389 \cdot 10^{-7}$
5	$-1.152 \cdot 10^{-5}$	$-7.09 \cdot 10^{-7}$	$-4.542 \cdot 10^{-8}$
6	$-1.494 \cdot 10^{-5}$	$-7.287 \cdot 10^{-7}$	$5.47 \cdot 10^{-6}$
7	$7.223 \cdot 10^{-7}$	$-2.386 \cdot 10^{-6}$	$2.706 \cdot 10^{-7}$
8	$1.461 \cdot 10^{-7}$	$9.369 \cdot 10^{-8}$	$-1.023 \cdot 10^{-7}$
9	$-2.433 \cdot 10^{-7}$	$-3.79 \cdot 10^{-7}$	$-1.377 \cdot 10^{-8}$

a

Part b)

$\Delta\phi := 0.9$	$\Delta\phi := 0.1$	$\Delta\phi := 0.5$
$-6.528 \cdot 10^{-7}$	$1.409 \cdot 10^{-5}$	$-5.432 \cdot 10^{-7}$
$-3.837 \cdot 10^{-5}$	$6.934 \cdot 10^{-5}$	$4 \cdot 10^{-6}$
$-9.847 \cdot 10^{-6}$	$2.359 \cdot 10^{-4}$	$4.832 \cdot 10^{-4}$
$-1.317 \cdot 10^{-5}$	$1.087 \cdot 10^{-3}$	$3.019 \cdot 10^{-5}$
$-2.824 \cdot 10^{-5}$	$1.777 \cdot 10^{-3}$	$1.921 \cdot 10^{-5}$
$9.007 \cdot 10^{-4}$	$6.016 \cdot 10^{-6}$	$7.922 \cdot 10^{-4}$
$2.81 \cdot 10^{-5}$	$9.999 \cdot 10^{-6}$	$1.798 \cdot 10^{-5}$
$6.479 \cdot 10^{-7}$	$5.639 \cdot 10^{-5}$	$7.213 \cdot 10^{-5}$
$4.713 \cdot 10^{-4}$	$2.392 \cdot 10^{-5}$	$1.427 \cdot 10^{-3}$
$-2.361 \cdot 10^{-4}$	$3.536 \cdot 10^{-5}$	$2.391 \cdot 10^{-4}$

b

Figure 7: The difference between the value of a) the quantities $U'_{m\sum k}$ / $U_{m.k}$ and b) φ_κ / $\angle C_k$

These analytical relations can be considered as a mathematical basis for the synthesis of methods for determining the phase shift of two harmonic signals using the spectral analysis of the signal obtained as a result of their addition after carrying out their two-half-cycle transformation. Further research should be directed to the development of intelligent diagnostic systems, which will be built based on algorithms of artificial intelligence, which, in turn, will reduce the time and increase the accuracy of measurements and forecasting the state of modern WME.

References

[1] O.M. Kryukov, R.S. Melnikov, V.A. Muzychuk, The method of diagnosing the technical condition of bores and ammunition based on the identification of the characteristics of the ballistic elements of the shot, Collection of scientific works of the National Academy 2(32) (2018) 5-11. doi:10.33405/2409-7470/2018/2/32/155166.

[2]   Y. V. Kuts, L. M. Shcherbak, Statistical phasometry. Ternopil State Technical University, 2009.

[3]   O.O. Lavrut, T.V. Lavrut, K.O. Klymovych, Yu.M. Zdorenko, The latest technologies and means of communication in the Armed Forces of Ukraine: the path of transformation and development prospects, Science and technology of the Air Force of the Armed Forces of Ukraine 1(34) (2019) 91-101. doi:10.30748/nitps.2019.34.13.

[4]   O.O. Lavrut, K.O. Klymovych, M.L. Tarasyuk, O.L. Antonyuk, Status and prospects of the use of modern technologies and means of radio communication in the Armed Forces of Ukraine Weapon, Systems and military equipment 1(49) (2017) 42-49.

[5]   L Bohdal, L. Kukiełka, S. Legutko, R. Patyk, A. M. Radchenko, Modeling and Experimental Research of Shear-Slitting of AA6111-T4 Aluminum Alloy Sheet, Materials 13(14) (2020) 3175. doi:10.3390/ma13143175.

[6]   F. Bonavolontà, M. D'Apuzzo, A. Liccardo, G. Mieleb, Harmonic and interharmonic measurements through a compressed sampling approach. Measurement 77 (2016) 1-15. doi:10.1016/j.measurement. 2015.08.022.

[7]   M.I. Skolnik, Radar Handbook. Third Edition. The McGraw-Hill Companies, 2008.

[8]   G. Sun, L. Wu, Z. Kuang, Z. Ma, J. Liu, Practical tracking control of linear motor via fractional-order sliding mode, Automatica 94 (2018) 221-235. doi:10.1016/j.automatica.2018.02.011.

[9]   Y. Wang, C. Wang, Y. Tao, Fast Frequency Acquisition and Phase Locking of Nonplanar Ring Oscillators, Appl. Sci. 7 (2017) 10-32. doi:10.3390/app7101032.

[10] S. Kihong, On the Selection of Sensor Locations for the Fictitious FRF based Fault Detection Method, International Journal of Emerging Trends in Engineering Research 7(7) (2019) 569-575. doi:10.30534/ijeter/2019/277112019.

[11] V.V. Pabyrivskyi, N.V. Pabyrivska, P.Y. Pukach, The study of mathematical models of the linear theory of elasticity by presenting the fundamental solution in harmonic potentials, Mathematical Modeling and Computing 7(2) (2020) 259–268.

[12] Yu. Kuts, A. Protasov, Y. Lycenco, O. Dugin, O. Bliznuk, V. Uchanin, Using Multidifferential Transducer for Pulsed Eddy Current Object Inspection, in Proceedings of IEEE First Ukraine Conference on Electrical and computer engineering (Ukrcon), May 29 –June 2, 2017. Kyiv, Ukraine, pp.826-829. doi:1109/UKRCON.2017.8100361

[13] S. A. Tyshko, V. G. Smolyar, O. E. Zabula, Analysis of the possibility of using two-half-period conversion for measuring the phase shift of harmonic signals with equal amplitude, Collection of scientific works of the Kharkiv University of the Air Force 2(30) (2013) 42-44.

[14] S. V. Gubin, S. O. Tyshko, O. E. Zabula, Yu. M. Chernychenko, Oscillographic method of phase shift measurement based on two-semi-periodic transformation, Radioelectronic and computer systems 4(2019) (2019) 47 – 54. doi:10.32620/reks.2019.4.05.

[15] S. Kihong, On the Selection of Sensor Locations for the Fictitious FRF based Fault Detection Method, International Journal of Emerging Trends in Engineering Research 7(7) (2019) 569-575. doi:10.30534/ijeter/2019/277112019.

[16] O. Klymovych, V. Hrabchak, O. Lavrut, T. Lavrut, V. Lytvyn, V. Vysotska, The Diagnostics Methods for Modern Communication Tools in the Armed Forces of Ukraine Based on Neural Network Approach, CEUR Workshop Proceedings 2631 (2020) 198-208.

[17] S. Tyshko, O. Lavrut, V. Vysotska, O. Markiv, O. Zabula, Y. Chernichenko, T. Lavrut, Compensatory Method for Measuring Phase Shift Using Signals Bisemiperiodic Conversion in Diagnostic Intelligence Systems, CEUR Workshop Proceedings 3312 (2022) 144-154.

[18] M. Nazarkevych, B. Yavourivskiy, I. Klyuynyk, Editing raster images and digital rating with software, in Proceedings of IEEE the Experience of Designing and Application of CAD Systems in Microelectronics, 2015, February, pp. 439-441.

[19] M. Nazarkevych, Y. Kynash, R. Oliarnyk, I. Klyujnyk, H. Nazarkevych, Application perfected wave tracing algorithm, in Proceedings of IEEE First Ukraine Conference on Electrical and Computer Engineering (UKRCON), 2017, May, pp. 1011-1014.

[20] M. Medykovskyy, P. Lipinski, O. Troyan, M. Nazarkevych, Methods of protection document formed from latent element located by fractals, in Proceedings of Xth International Scientific and Technical Conference on Computer Sciences and Information Technologies (CSIT), 2015, September, pp. 70-72.

[21] V. Motyka, M. Nasalska, Y. Stepaniak, V. Vysotska, M. Bublyk: Radar Target Recognition Based on Machine Learning, CEUR Workshop Proceedings 3373 (2023) 117-128.

[22] L. Mochurad, R. Bliakhar, N. Reverenda, Identification and Tracking of Unmanned Aerial Vehicles Based on Radar Data, CEUR Workshop Proceedings 3426 (2023) 171-181.

[23] A. Vasyliuk, T. Basyuk, V. Lytvyn. Specialized interactive methods for using data on radar application models, CEUR Workshop Proceedings 2631 (2020) 1–11.

[24] I.N. Garkusha, V.V. Hnatushenko, V. V. Vasyliev, Research of influence of atmosphere and humidity on the data of radar imaging by Sentinel-1, in Proceedings of IEEE 37th International Conference on Electronics and Nanotechnology (ELNANO), Kiev, 2017, pp. 405-408. doi: 10.1109/ELNANO.2017.7939787.

[25] V. Hnatushenko, I. Garkusha, V. Vasyliev, Creating soil moisture maps based on radar satellite imagery, Proceedings of SPIE 10426, Active and Passive Microwave Remote Sensing for Environmental Monitoring, 104260J, 3 October 2017. doi:10.1117/12.2278040.

[26] O. Kavats, V. Hnatushenko, Y. Kibukevych, Y. Kavats, Flood Monitoring Using Multi-temporal Synthetic Aperture Radar Images, Advances in Intelligent Systems and Computing 1080 (2020) Springer, Cham. doi:10.1007%2F978-3-030-33695-0_5

[27] M. Makaruk, A. Nazarov, I. Shubin, N. Shanidze, Knowledge Representation Method for Object Recognition in Nonlinear Radar Systems, CEUR Workshop Proceedings 2870 (2021) 948-958.

[28] V. Lytvyn, V. Vysotska, I. Peleshchak, I. Rishnyak, R. Peleshchak, Time Dependence of the Output Signal Morphology for Nonlinear Oscillator Neuron Based on Van der Pol Model, International Journal of Intelligent Systems and Applications 10 (2018) 8-17. doi:10.5815/ijisa.2018.04.02.

[29] A. Semenov, et al., Signal Statistic and Informational Parameters of Deterministic Chaos Transistor Oscillators for Infocommunication Systems, in Proceedings of International Scientific-Practical Conference on Problems of Infocommunications Science and Technology, PIC S and T, 2019, pp. 730–734.

[30] A.O. Semenov, A.Y. Savytskyi, O.V. Bisikalo, P.I. Kulakov, Mathematical modeling of the two-stage chaotic colpitis oscillator, in Proceedings of 14th International Conference

on Advanced Trends in Radioelectronics, Telecommunications and Computer Engineering, TCSET, 2018, April, pp. 835–839.

[31] O. Soprun, M. Bublyk, Y. Matseliukh, V. Andrunyk, L. Chyrun, I. Dyyak, A. Yakovlev, M. Emmerich, O. Osolinsky, A. Sachenko, Forecasting Temperatures of a Synchronous Motor with Permanent Magnets Using Machine Learning, CEUR workshop proceedings 2631 (2020) 95–120.

[32] M. Zagirnyak, O. Chorna, O. Bisikalo, O. Chornyi, A model of the assessment of an induction motor condition and operation life, based on the measurement of the external magnetic field, in Proceedings of IEEE 3rd International Conference on Intelligent Energy and Power Systems, IEPS, 2018, January, pp. 316–321.

[33] A. Podorozhniak, N. Liubchenko, M. Kvochka, I. Suarez, Usage of intelligent methods for multispectral data processing in the field of environmental monitoring, Advanced Information Systems 5(3) (2021) 97–102. doi:10.20998/2522-9052.2021.3.13.

[34] R. R. Imanov, A. A. Bayramov, Development of field signal centers based on the modern telecommunication technologies. Advanced Information Systems 4(1) (2020) 136–139. doi:10.20998/2522-9052.2020.1.21.

[35] T. Toosi, M. Sirola, J. Laukkanen, M. van Heeswijk, J. Karhunen, Method for detecting aging related failures of process sensors via noise signal measurement, International Journal of Computing 18(2) (2019) 135-146.

[36] A.B. Lozynskyy, I.M. Romanyshyn, B.P. Rusyn, Intensity Estimation of Noise-Like Signal in Presence of Uncorrelated Pulse Interferences, Radioelectronics and Communications Systems 62(5) (2019) 214–222.

[37] K. Smelyakov, M. Volk, I.Ruban, M. Derenskyi, A. Chupryna, Short-Range Navigation Radio System Simulator, CEUR Workshop Proceedings 3403 (2023) 539-554.

[38] R.M. Peleshchak, O.V. Kuzyk, O.O. Dan'kiv, Non-linear model of impurity diffusion in nanoporous materials upon ultrasonic treatment, Condensed Matter Physics 17(2) (2014) 23601.

[39] R.M. Peleshchak, O.V. Kuzyk, O.O. Dan'kiv, Formation of periodic structures under the influence of an acoustic wave in semiconductors with a two-component defect subsystem, Ukrainian Journal of Physics 61(8) (2016) 741-746.